Journal of Integrated
SCIENCE & TECHNOLOGY

Optimal direction of arrival estimation for digital beamforming using machine learning

Sachin Bandewar,* Virendra S. Chaudhary

Department of Electronics and Communication Engineering, RKDF University, Bhopal, India.

Received on: 28-Sep-2023, Accepted and Published on: 12-Dec-2023

Article

ABSTRACT

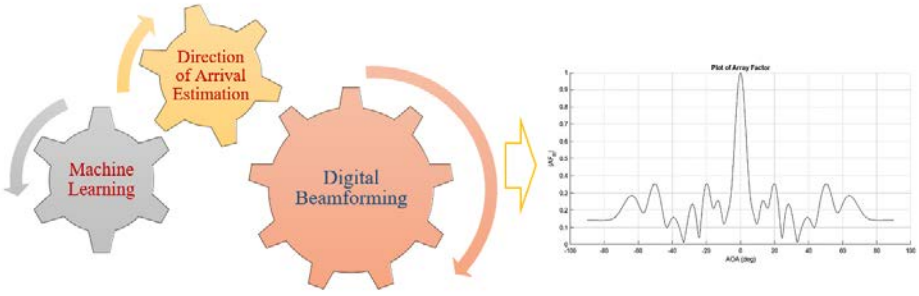

Smart antenna systems play a pivotal role in modern wireless communication by dynamically adjusting antenna radiation patterns to enhance signal reception or transmission. This paper explores the application of adaptive algorithms and machine learning techniques in optimizing the direction of arrival (DOA) estimation for smart antennas. We review related work in the field, including studies on antenna design, gain enhancement, and multiple-input multiple-output (MIMO) systems. The methodology section details the use of algorithms such as Least Mean Squares (LMS) and Long Short-Term Memory (LSTM) networks to improve DOA estimation and beamforming. Our extensive result analysis demonstrates the effectiveness of these algorithms in various scenarios, including different numbers of antennas and angles of signal arrival. Through AOA analysis, we highlight how machine learning and deep learning techniques can significantly enhance the capabilities of smart antenna systems, making them adaptable to diverse signal environments.

Keywords: Smart Antenna, Adaptive Beamforming, Direction of Arrival (DOA), Machine Learning, Deep Learning

INTRODUCTION

In a smart antenna system, the radiation pattern of the antenna is adjusted using specific algorithms processed by digital signal processors. The inputs to these antenna arrays consist of the desired signal, interfering signals, and Gaussian noise. Through adaptive algorithms, the weights of the array are fine-tuned, leading to a reduction in the output error.[1]

This error is derived by subtracting the output signal from a reference signal. By optimizing the adaptive algorithms, one can control this error by adjusting the weights. A well-designed adaptive algorithm can either maximize or minimize the signal-to-interference ratio, depending on various optimization criteria such as variance, mean squared error (MSE), interference nulling, and directing the main beam towards the user. Two key components of the smart antenna system are the estimation of the direction of arrival (DOA) and digital beamforming (DBF).[2] The Direction of Arrival (DOA) is alternatively referred to as spectral estimation, bearing estimation, or Angle of Arrival (AOA) estimation. When dealing with adaptive array processing, if multiple transmitters are functioning simultaneously, each transmitter creates numerous propagation paths and AOAs at the receiving end.[3]

As a result, the antenna array is tasked with discerning the accurate AOA by filtering out interference and noise signals to achieve higher fidelity. An M-element array consists of "M" potential weights and "N" incoming plane waves from "N" in different directions, with the condition that N<M. Each of these waves includes adaptive white Gaussian noise (AWGN).
The output of the array can be represented as follows:

$$y(t) = \bar{W} * \bar{Z}(t) \quad (1)$$

where $\bar{W} = [w_1, w_2, \ldots . w_n]$ array weights, $\bar{Z}(t)$= incident signals vector.

Smart antennas can be broadly categorized into two types: the Switched Beam Antenna and the Adaptive Beamforming.

*Corresponding Author: Sachin Bandewar
Email: sachin.bandewar9@gmail.com

Cite as: *J. Integr. Sci. Technol., 2024, 12(3), 771.*
URN:NBN:sciencein.jist.2024.v12.771

As per various literature sources, a switched-beam system selects from a set of predefined patterns to enhance the received signal quality. Upon detecting an incoming signal, the base station identifies which beam is best aligned with the direction of the signal of interest. The system then switches to the optimal beam for communication with the user. This approach, while simpler and faster, offers limited flexibility as the system is constrained by predefined patterns.

Contrary to the switched-beam system, an adaptive array offers a virtually infinite number of patterns. These patterns are dynamically adjusted in real time based on the prevailing radio environment, i.e., the channel condition. This type of array consists of multiple antenna elements. It continually modifies its radiation pattern based on feedback from the surrounding environment, ensuring that the array always operates in an optimal state.

When the angles of the desired signals vary over time, it's crucial to have a mechanism that can persistently update the array weights. This is where adaptive beamforming shines, as it can track mobile users consistently in a changing RF environment. Some of the adaptive beamforming, are such as LMS (Least Mean Squares), NLMS (Normalized Least Mean Squares), and RLS (Recursive Least Squares).

RELATED WORK

Salhane, M. et al.[1] developed the gain of a smart antenna from 4×4 to multiple patches. In this study, we have developed a sensitive smart switched beam multiple patch antenna system at the 5.8 GHz frequency. To achieve this system, we first optimized and validated a two-element patch antenna array. To provide the necessary phase shift between the antenna elements to fit the radiation pattern, we have designed and built a smart switching beam antenna based on analog beamforming technology. It is a spatial filtering design using the Butler matrix. To improve the transmission system and increase its ability to serve targets in an optimal and directive way, an intelligent system based on a 4×4 planar Butler array connected to eight patch antennas has been designed. The proposed system has a very high gain of the order of 74.41 dB around the resonant frequency compared to a smart antenna with four patches, whose gain is equal to 17.98 dB.

R. Ullah et al.[2] presented an eight-element array antenna with a single-layer frequency selective surface (FSS) to obtain high gain. The eight elements are fed by a single port. The FSS consists of 14 × 6 unit cells with one unit cell size is 5 × 5 mm 2 having wideband behavior. The eight-element antenna integrated with the FSS reflector, which results in an improvement in the gain level from 12 dB to 15 dB at 28 GHz, from 10 dB to 12 dB at 38 GHz, and from 9.5 to 11 dB at 60 GHz. The dimensions of the antenna are 65 × 27 × 0.857 mm 3. The proposed antenna shows stable gain and directional radiation patterns. The simulation findings are experimentally confirmed, by testing the fabricated prototypes of the proposed antenna system.

X. L. Chang et al.[3] described for the first time, that the ionic polymer metal composite (IPMC) actuator is integrated with a radio frequency identification (RFID) tag antenna for achieving frequency reconfiguration in the ultrahigh-frequency (UHF) band. Here, the IPMC movable flap serves as an actuator that can effectively tune the tag resonant frequency. Numerical and experimental data confirm that the tip displacement of the IPMC actuator can be enhanced up to 266% with the use of the two-layer-crenelated structure. The IPMC actuator allows the resonant frequency of the tag antenna to be tuned back by as much as 35 MHz, after deviating due to placing on an unintended object. UHF RFID application is also performed using a portable commercial RFID reader. Good frequency reconfiguration and broad tuning range, along with far-read distances, have been achieved with our tunable UHF RFID tag antenna.

Vidya P. et al.[4] presented the design of an 8-element linear array for Adaptive Antenna applications using the Least Mean Square (LMS) algorithm towards improving the directive gain, beam steering capabilities, half-power beam width, sidelobe level, and bandwidth of array. A conventional patch antenna is optimized to operate at 3.6 GHz (5G applications) with two symmetrical slots and a Quarter Wave Transformer for feeding, and this design is extended up to 8 elements using CST Microwave Studio parameterization. The Return Loss (S11), Directivity, HPBW, and VSWR of the antenna array are observed for the 2, 4, and 8-element adaptive arrays. Further, the LMS algorithm is used to compute the optimal complex weights, considering different angles for the desired User (+45˚ and -45˚) and Interferer (+20˚ and -20˚) during MATLAB simulation, and then these optimal weights are fed to antenna elements using CST for beam steering in a different direction. Maximas in the direction of the user and nulls in the direction of the interferer are obtained using CST software and found closely matching with MATLAB results.

R. Ullah, S. et al.[5] presented a 10-port, hybrid multiple-input multiple-output (MIMO) antenna system for 5G Smartphone applications. The overall dimensions of the proposed antenna system are 150 × 80 mm 2. The proposed antenna system is fabricated and tested. Experimental results show reflection coefficients better than -6 dB and -10 dB for multi-band and single-band modules, respectively, with high isolation levels between the antenna elements in both modules. Moreover, the measured envelope correlation coefficients (ECC) are well below 0.3 and 0.1 for the proposed multi-band and single-band modules, respectively. In addition, single antenna elements in both modules show good radiation characteristics with maximum peak gain between 2 dBi and 4 dBi. Finally, 43 bps/Hz channel capacity is achieved in the single-band module. With these characteristics, the proposed antenna system can be a good candidate for modern mobile communication systems.

N. Shoaib et al.[6] presented the design of 8×8 multiple-input multiple-output (MIMO) antennas for future 5G devices, such as smartwatches and dongles. Each antenna is fed from the bottom layer of the substrate through vias to avoid any spurious radiation. The MIMO antennas resonate at 25.2 GHz with a 6-dB percentage bandwidth of 15.6%. The gain attained by the antennas in the entire bandwidth is above 7.2 dB with a maximum value of 8.732 dB at the resonant frequency. Likewise, the value of efficiency attained by the antennas in the entire bandwidth is above 65% with a maximum value of 92.7% at the resonant frequency. The simulation and measurement results have substantiated the good performance

of the MIMO antennas, thus making them suitable for compact 5G devices.

S. H. Kiani, et al.[7] discussed in this work, a simple, low-cost, dual wideband sub6GHz Multiple Input Multiple Output (MIMO) antenna system for a smartphone is presented. The antenna system is fabricated using an inexpensive and commercially easily available 0.8 mm thick FR4 substrate. The presented system consists of a single main board and two side boards containing eight antennas and feedings. The radiating elements are etched on the side boards to provide space for other electronic components RF systems and sub-systems. Moreover, various key performance parameters such as envelope correlation coefficient (ECC), mean effective gain (MEG), channel capacity (CC), specific absorption rate (SAR), gain, and efficiency are also presented. It is found that the peak gain of the system is 5.8 dBi, ECC is lower than 0.015, efficiency ranges between 58% to 78%, peak SAR is 1.28 W/Kg, and the maximum CC is 40.2 bps/Hz within the frequency band of interest. In addition, to further demonstrate the usefulness of such a structure as a smart mobile terminal, single and dual-hand scenarios are also presented.

Y. -Y. Wang et al.[8] discussed A dual-loop antenna with massive-input–massive-output (MIMO) operation within the fourth-generation Long Term Evolution (LTE) bands for smart glasses applications is proposed. For each single-loop antenna to excite four resonant modes so that it can yield a desirable −6 dB impedance matching across the desired low band (LB), 824–960 MHz, and high band (HB), 1710–2690 MHz, of LTE operations, a simple matching circuit is loaded into the open section of the loop antenna. Further measurements show good efficiency and isolation across the LB and HB for the dual-loop antenna. Finally, the calculated envelope correlation coefficient and ergodic channel capacity of the 2 × 2 MIMO antenna are also discussed.

L. Sun et al.[9] presented a wideband orthogonal-mode dual-antenna pair with a shared radiator for fifth-generation (5G) multiple-input multiple-output (MIMO) metal-rimmed smartphones. By arranging four such dual-antenna pairs at two side edges of the smartphone, an 8 × 8 MIMO system is fulfilled. Both the simulation and measurement results show that the proposed 8 × 8 MIMO system could offer an isolation of better than 12.0 dB and an envelope correlation coefficient of lower than 0.11 between all ports. The measured average antenna efficiencies are 74.7% and 57.8% for the two antenna elements of the dual-antenna pair. We portend that the proposed design scheme, with the merits of the shared radiator, wide bandwidth, and metal rim compatibility, has the potential for the application of future 5G smartphones.

M. Usman et al.[10] described In this article, a compact dual-port single-element MIMO antenna is presented for millimeter wave (mmWave) 5G wireless applications. The presented antenna design consists of an annular ring slot that is fed by a Substrate Integrated Waveguide (SIW) at the two opposite sides of the substrate. The antenna resonates at 28GHz and its 10dB impedance bandwidth is 400MHz. The isolation between the ports is reduced by introducing an additional annular slot that acts as a cavity which results in an isolation better than 20dB at 28GHz. The measured gain of both ports is 6.9 dBi which is the highest gain per unit element at 28GHz in the literature. The measured diversity gain and envelope correlation coefficient are 9.98dB and 0.065, respectively, at the band of interest. The measured and simulated results are in good agreement.

Mohapatra et al.[11] presented an improved LMS algorithm for tap detection in communication systems, showing enhanced convergence rate and bandwidth efficiency through simulation.

Romeu et al.[12] developed a 16-beam lens antenna for 5G systems, offering wide coverage and high performance in specific frequency ranges.

Wei et al.[13] demonstrated how attackers can exploit programmable metasurfaces in passive and active modes to intercept or manipulate wireless communications, highlighting security risks in next-gen networks.

Dinesh Kumar et al.[14] proposed a proactive flow control technique for Wireless Network-on-Chip, using adaptive beamforming and fuzzy logic for efficient data traffic management and improved QoS.

Ranjeet Yadav et al.[15] enhanced 5G beamforming using 3D-MIMO and SVM, achieving better throughput and SNR, addressing challenges in dense user environments.

Biswas et al.[16] improved bandwidth using stacked DRA antennas, showing significant enhancement with air gap introduction.

Komeylian et al.[17] implemented LCMV beamforming for cylindrical antenna arrays, achieving high efficiency and signal resolution in digital wireless communications.

Shome et al.[18] created a miniaturized quad-element MIMO antenna for IoT applications using UWB technology, achieving high performance with low mutual coupling.

Bandewar et al.[19] focused on improving communication modules for digitalization in smart environments, experimenting with different PCB antenna designs.

Aboualalaa et al.[20] proposed a multi-band rectenna for IoT, combining energy harvesting and data communication capabilities.

Jabbar et al.[21] explored the potential of 60 GHz mmWave technology for URLLC in industrial applications, emphasizing its importance in Industry 4.0.

METHODOLOGY USED

Optimal Direction of Arrival (DOA) estimation is a critical aspect of digital beamforming. By accurately determining the DOA, a system can focus its resources and attention in the direction of the desired signal, enhancing performance and minimizing interference. With the rise of machine learning (ML) techniques, there's a growing interest in leveraging these methods to improve DOA estimation. The flowchart of the proposed methodology is presented in figure 1.

Adaptive beamforming, which involves adjusting the phases and amplitudes of signals in an antenna array to improve signal reception or transmission in specific directions, can benefit significantly from the application of machine learning (ML) algorithms. Traditional algorithms like Least Mean Squares (LMS) have been foundational, but with the advent of machine learning, there's potential for significant enhancement.

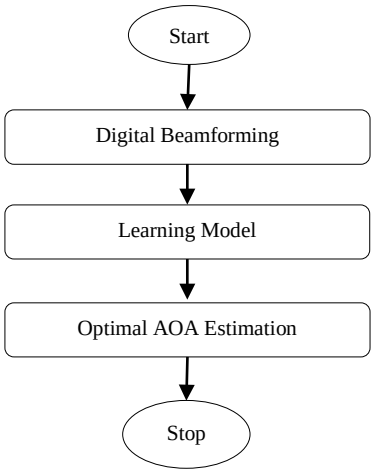

Figure 1. Flowchart of design

Digital Beamforming using Machine Learning

The Least Mean Squares (LMS) algorithm, which is adaptive by nature, has been a primary method for weight calculation in beamforming. By using LMS as a basis, you can develop a dataset capturing the relationship between input signals and the optimal weights determined by LMS.

Array Factor Optimization Using ANN

Artificial Neural Networks (ANN) can be employed to model complex relationships. In the context of beamforming:

The ANN can be trained on the dataset generated using LMS to predict weights for different inputs. The flexibility of ANN allows it to adjust its learning rate, potentially leading to faster and more accurate weight prediction compared to traditional LMS. Once trained, the ANN model can quickly determine optimal weights for incoming signals without needing iterative weight adjustments like traditional LMS.

A Multilayer Perceptron (MLP) is a type of feedforward artificial neural network (ANN), as presented in figure 2.

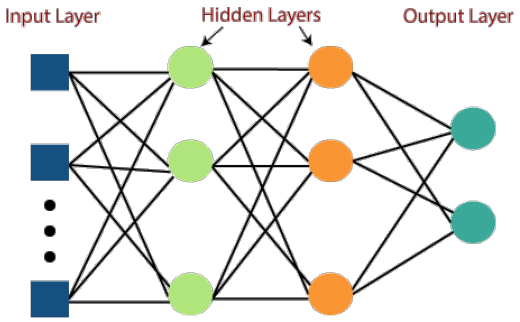

Figure 2. ANN Architecture [22]

Here's a basic overview:

Input Layer: This is where you feed your data into the network. The number of neurons in this layer corresponds to the number of input features.

Hidden Layers: An MLP can have one or multiple hidden layers. Each neuron in a hidden layer is a linear combination of the outputs from the previous layer, passed through a non-linear activation function.

Output Layer: The final layer, where the result is produced. For regression tasks, there's typically one neuron. For classification tasks, there might be multiple neurons (one for each class), especially if it's a multi-class problem.

Activation Functions: Common activation functions include the sigmoid, hyperbolic tangent (tanh), and ReLU (rectified linear unit). The activation function introduces non-linearity into the model, enabling it to learn complex relationships.

Backpropagation: It's the algorithm used to train MLPs. During training, the error between the predicted outputs and the true outputs is calculated and then propagated back through the network to update the weights.

Training: The training of an MLP typically involves defining a loss function (like mean squared error for regression or cross-entropy for classification) and then using an optimization algorithm (like gradient descent) to adjust the weights and biases in the network to minimize the loss.

While MLPs are foundational and can solve a wide array of problems, specialized neural network architectures are often preferred for specific problem domains.

Array Factor Optimization using Deep Learning

Long Short-Term Memory (LSTM) networks, a type of recurrent neural network (RNN), are well-suited for sequences and time-series data. Given the temporal nature of signals, LSTM can capture long-term dependencies in the data, making it apt for predicting weights based on a sequence of past signals. By adding regression layers after LSTM layers, the network can be tailored to predict continuous values, like the weights in beamforming. This deep learning model can be trained on sequences of input signals and their corresponding optimal weights (determined by LMS or another method) to predict weights for new sequences of input signals.

LSTM models are a sort of recurrent neural network RNN that may learn order dependency in sequence prediction challenges. This is a need in a variety of complicated issue areas, including machine translation, voice commands, and others. LSTMs interact including both Long Term Memory (LTM) as well as Short Term Memory (STM), and the notion of gates is used to make the computations normally effective and efficient.

Forget Gate: When LTM enters the forget gate, it discards information that is no longer helpful.

Learn Gate: The event (current inputs) with the STM is merged such that the relevant information from the STM may be used upon the current input.

Remember Gate: LTM information one which we don't want to forget, as well as STM with Event information, were also merged in Remember Gate, which functions as the latest LTM.

Use Gate: This gate predicts the outcome of the current event using LTM, STM, and Event, and acts as an upgraded STM.

Deep learning's LSTMs are a complicated topic.

The first segment determines whether the information from the preceding timestamp is significant and should be remembered or ignored. The cell attempts to learn new valuable learning from the

input in the second section. Finally, the cell sends new information from the current and then to the next timestamp in component number 3. The gates are the 3 components of an LSTM cell. The Forget gate is the very first section, the Input gate second one then the Output gate is the last one i.e. third one.

Long-Short Term Memory (LSTM) is an acronym for Long-Short Term Memory. In terms of memory, LSTM is a sort of Recurrent neural network RNN that outperforms standard RNN. LSTMs behave far better when it comes to learning specific patterns.

An LSTM, like a basic RNN, contains a hidden state, with H(t-1) representing the former timestamp's hidden state where Ht shows the present timestamp's hidden state. LSTMs also contain a cell state, which is expressed by C(t-1) and C(t), accordingly, for past and current timestamps. STM refers to the hidden state, whereas LTM refers to the cell state. Take a look at the illustration below.
It's worth noting that the cell state contains all of the information as well as all of the timestamps.

The initial step in an LSTM network cell is to select either to retain or discard the information out of the preceding timestamp. This forgets gate equation is as follows.

$$f_t = \sigma\left(X_t * U_f + H_{t-1} * W_f\right) \quad (2)$$

Here
Xt: input to the current timestamp.
Uf: weight associated with the input
Ht-1: The hidden state of the previous timestamp
Wf: It is the weight matrix associated with the hidden state
A sigmoid function is then applied to it. As a result, it will be a value between 0 & 1.

Furthermore, LSTM is a modern, improved division that solves the issue of long-term dependency. Despite this, RNN predicts the present state using the stored data as information from the past. Whenever the gap between the present state and the prior state from which the information must be gathered is considerable, it fails to connect the information. Four layers in the network are employed.
An amplitude value is supplied into the LTSM cell for every timestep, which therefore quantifies the hidden vector and sends it on to another timestep. Depending on the latest current input at the usual recent hidden vector ht-1, the currently hidden vector of timestep ht is calculated. That is how a RNN captures sequential information:

LSTM can be used for classification similar to how you would use other network architectures such as CNN or Connected networks for classification: By appending a final fully connected layer to the LSTM, with the number of classes being the output dimension of the fully connected layer and training the entire network with a cross-entropy loss.

In terms of the inputs to the final fully-connected layer, that depends on your applications. We can send the states from just the last LSTM cell or concatenate states from multiple LSTM cells. Finally, we would use an LSTM for classification only if we have sequential data and believe that our data's temporally correlated features are useful for classifying your sequential data.

RESULT ANALYSIS

In Figure 3 AOA analysis is presented for the NLMS algorithm with 5 antennas. The x-axis represents AOA and the y-axis represents amplitude. The study evaluated the amplitude response of a beamforming algorithm by varying the number of antenna elements and the distance between them. The precise positions of these peaks may vary slightly due to the different algorithms in use. Figure 4 shows an AOA analysis for a machine learning algorithm with 5 antennas that effectively detects and responds to signals from different directions. This behavior is typical of an adaptive beamforming system, which can focus its reception or transmission capabilities in multiple directions based on the incoming signal environment.

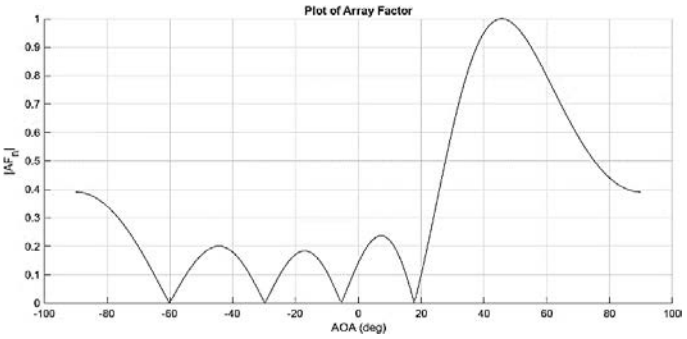

Figure 3. AOA Analysis for NLMS Algorithm with 5 Antennas

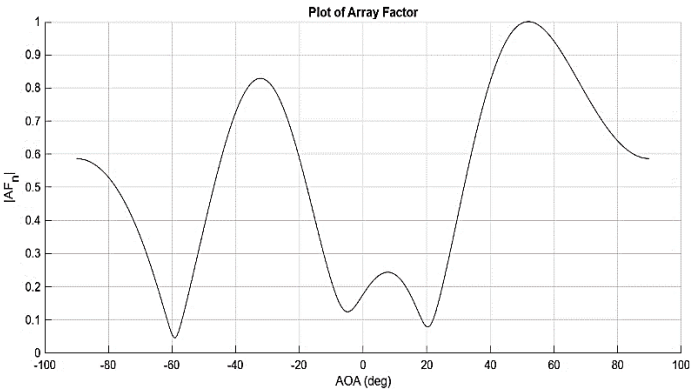

Figure 4. AOA Analysis for ML Algorithm with 5 Antennas

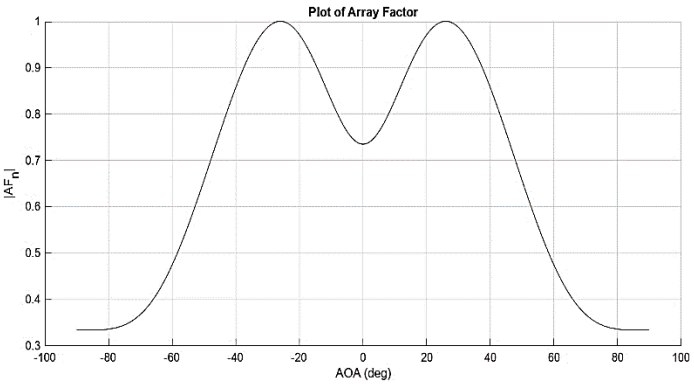

Figure 5. AOA Analysis for Deep Learning Algorithm with 5 Antennas

Figure 5 shows AOA analysis for deep learning algorithm with 5 antennas. This behavior is typical of an adaptive beamforming

system, which can focus its reception or transmission capabilities in multiple directions based on the incoming signal environment.

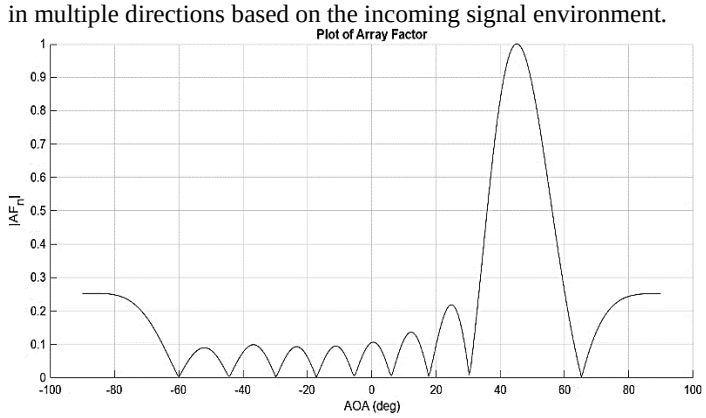

Figure 6. AOA Analysis for NLMS Algorithm with 10 Antennas

Figure 6 shows AOA analysis for the NLMS algorithm with 10 antennas that effectively detect and respond to signals from different directions. Figure 7 shows AOA analysis for an ML algorithm with 10 antennas that effectively detects and responds to signals from different directions. Figure 8 shows AOA analysis for the DL algorithm with 10 antennas that effectively detect and respond to signals from different directions. Figure 9 shows AOA analysis for the NLMS algorithm with 15 antennas that effectively detect and respond to signals from different directions. Figure 10 shows AOA analysis for an ML algorithm with 15 antennas that effectively detects and responds to signals from different directions.

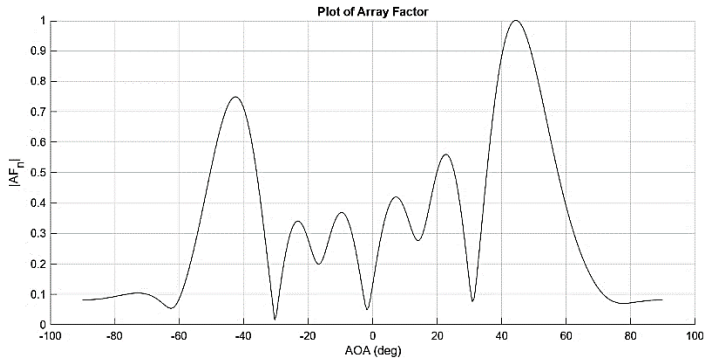

Figure 7. AOA Analysis for ML Algorithm with 10 Antennas

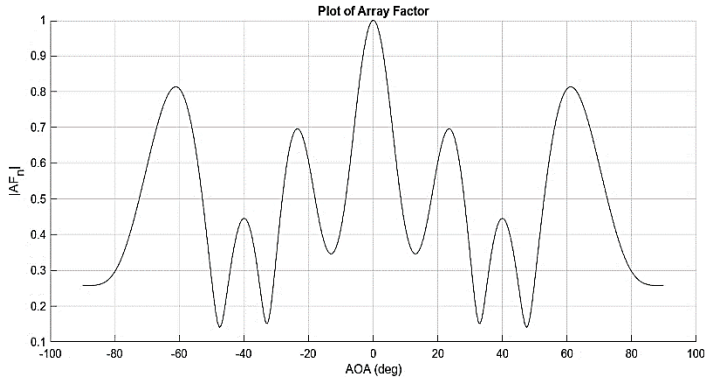

Figure 8. AOA Analysis for DL Algorithm with 10 Antennas

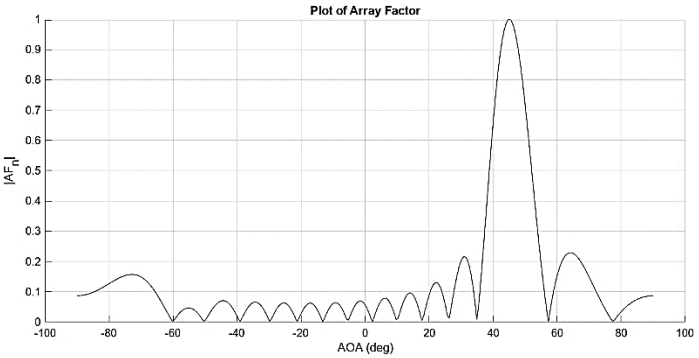

Figure 9. AOA Analysis for NLMS Algorithm with 15 Antennas

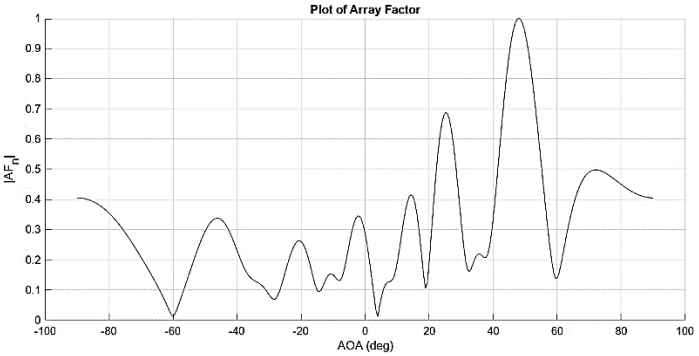

Figure 10. AOA Analysis for ML Algorithm with 15 Antennas

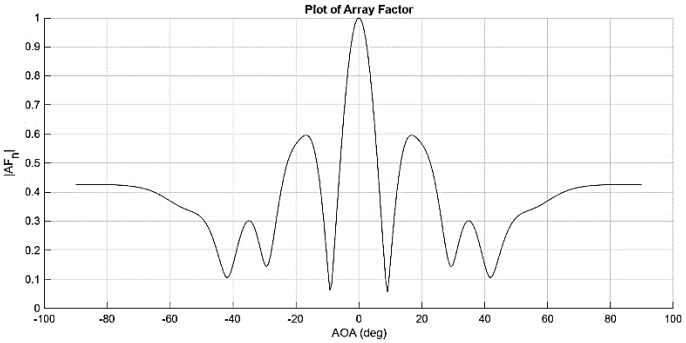

Figure 11. AOA Analysis for DL Algorithm with 15 Antennas

Figure 11 shows AOA analysis for the DL algorithm with 15 antennas that effectively detect and respond to signals from different directions.

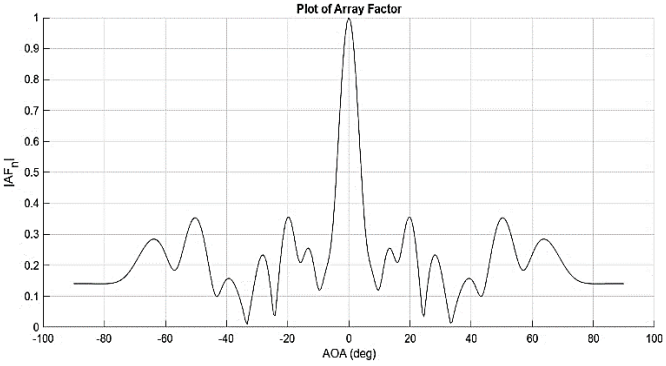

Figure 12. AOA Analysis for NLMS Algorithm with 20 Antennas

Figure 12 shows AOA analysis for the NLMS algorithm with 20 antennas that effectively detects and responds to signals from different directions.

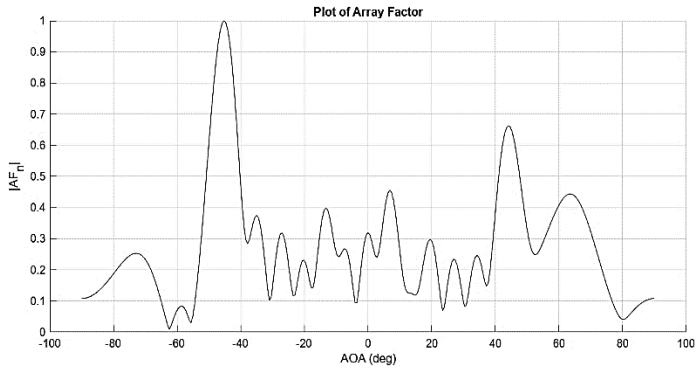

Figure 13. AOA Analysis for ML Algorithm with 20 Antennas

Figure 13 shows an AOA analysis for an ML algorithm with 20 antennas that effectively detects and responds to signals from different directions.

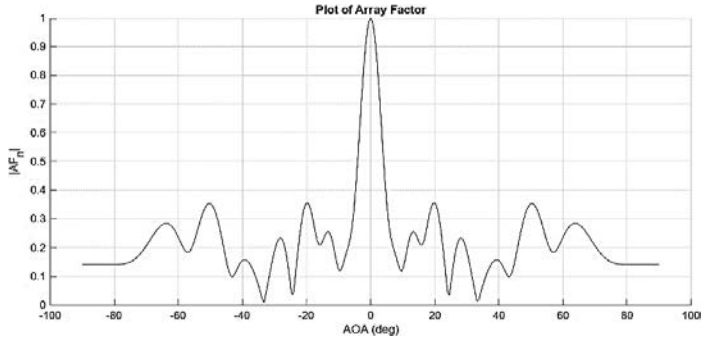

Figure 14. AOA Analysis for DL Algorithm with 20 Antennas

Figure 14 shows AOA analysis for the DL algorithm with 20 antennas that effectively detect and respond to signals from different directions.

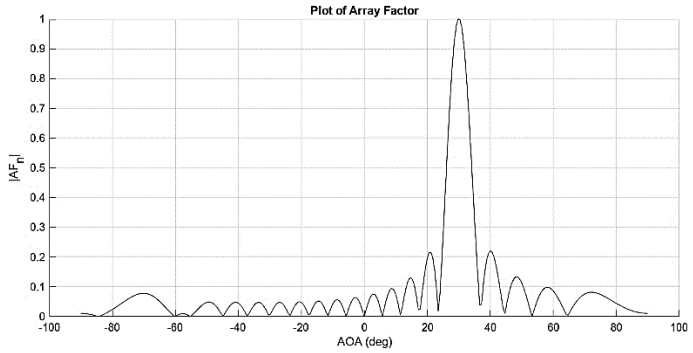

Figure 15. AOA Analysis for NLMS Algorithm with **30°** Antennas Angle

Figure 15 shows AOA analysis for the NLMS algorithm with 30° antenna angle that effectively detects and responds to signals from different directions.

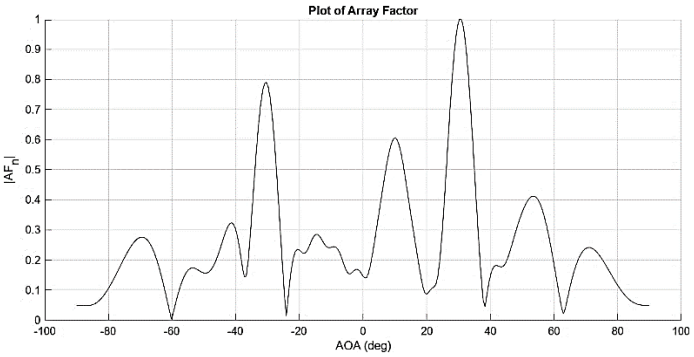

Figure 16. AOA Analysis for ML Algorithm with **30°** Antennas Angle

Figure 16 shows AOA analysis for ML algorithm with 30° antennas angle that effectively detects and responds to signals from different directions.

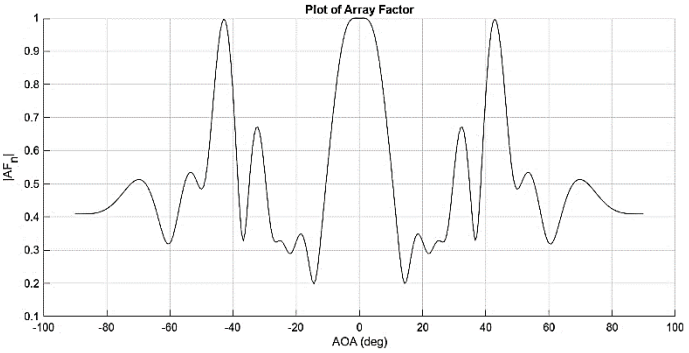

Figure 17. AOA Analysis for DL Algorithm with **30°** Antennas Angle

Figure 17 shows AOA analysis for DL algorithm with 30° antennas angle that effectively detects and responds to signals from different directions.

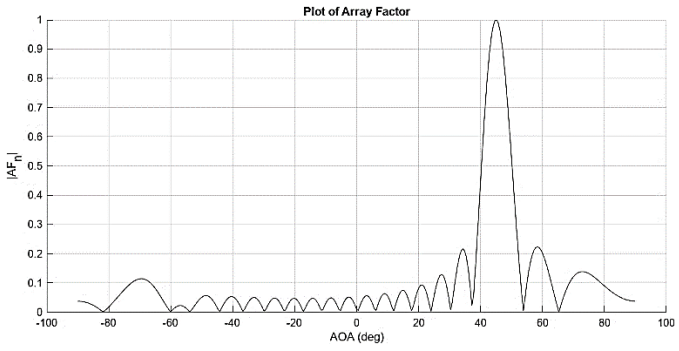

Figure 18. AOA Analysis for NLMS Algorithm with **45°** Antennas Angle

Figure 18 shows AOA analysis for the NLMS algorithm with 45° antenna angle that effectively detects and responds to signals from different directions. Figure 19 shows AOA analysis for the ML algorithm with 45° antenna angle that effectively detects and responds to signals from different directions.

Figure 20 shows AOA analysis for the DL algorithm with 45° antenna angle that effectively detects and responds to signals from different directions.

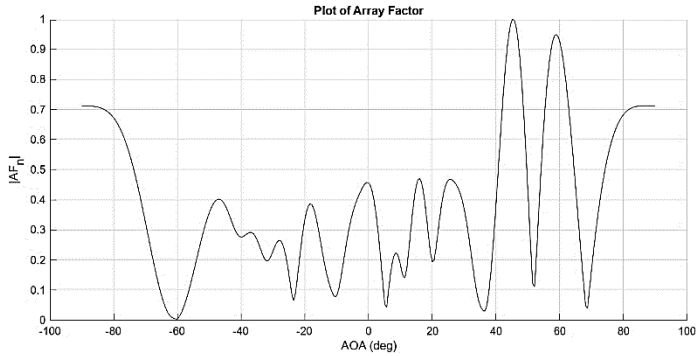

Figure 19. AOA Analysis for ML Algorithm with **45°** Antennas Angle

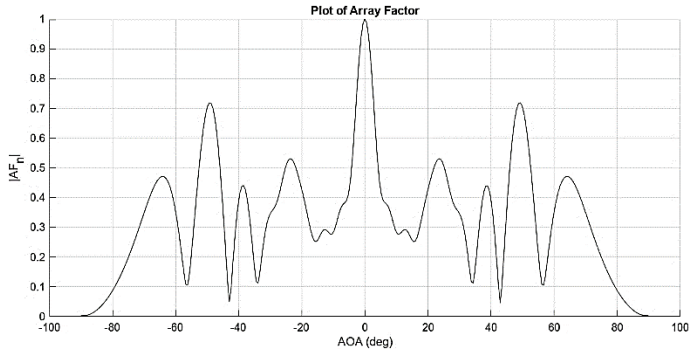

Figure 20. AOA Analysis for DL Algorithm with **45°** Antennas Angle

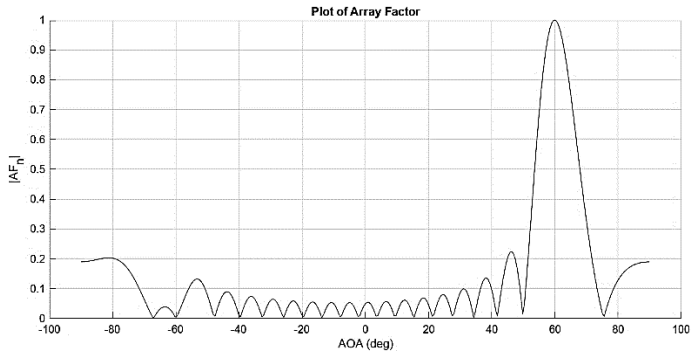

Figure 21. AOA Analysis for NLMS Algorithm with **60°** Antennas Angle

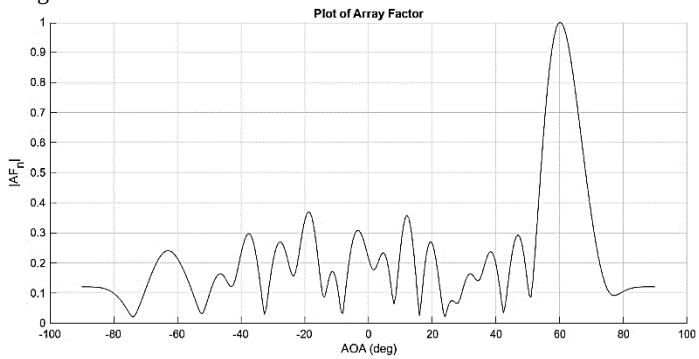

Figure 22. AOA Analysis for ML Algorithm with **60°** Antennas Angle

Figure 22 shows AOA analysis for an ML algorithm with 60° antenna angle that effectively detects and responds to signals from different directions.

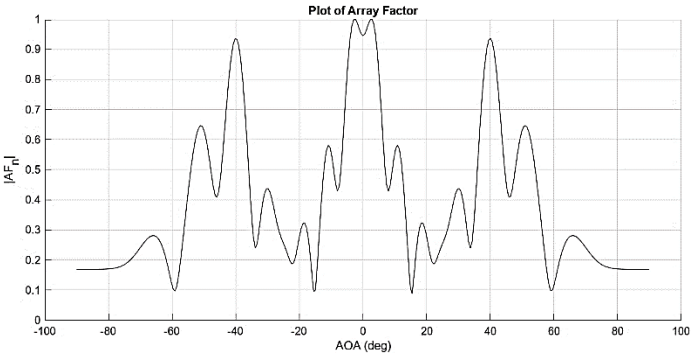

Figure 23. AOA Analysis for DL Algorithm with **60°** Antennas Angle

Figure 21 shows AOA analysis for the NLMS algorithm with 60° antenna angle that effectively detects and responds to signals from different directions.

Figure 23 shows AOA analysis for the DL algorithm with 60° antenna angle that effectively detects and responds to signals from different directions.

The series of AOA (Angle of Arrival) analyses across various figures demonstrates the effectiveness of NLMS, ML, and DL algorithms in adaptive beamforming systems. Each algorithm, applied with varying numbers of antennas (5, 10, 15, 20) and at different antenna angles (30°, 45°, 60°), consistently shows the capability to effectively detect and respond to signals from multiple directions. This indicates the robustness and adaptability of these algorithms in handling diverse signal environments, regardless of the number of antennas or their orientation, which is crucial for efficient wireless communication systems.

CONCLUSION

In the era of advanced wireless communication, smart antenna systems stand as key enablers for achieving high-quality signal reception and transmission. This study has shed light on the potential of adaptive algorithms and machine learning techniques to optimize the direction of arrival (DOA) estimation, a critical aspect of smart antenna operation. By reviewing related work, we observed the ongoing efforts to improve antenna design, gain enhancement, and MIMO systems in the field. Our methodological exploration highlighted the effectiveness of algorithms such as Least Mean Squares (LMS) and Long Short-Term Memory (LSTM) networks in enhancing DOA estimation and adaptive beamforming. The comprehensive AOA analysis showcased the remarkable capabilities of machine learning and deep learning algorithms in adapting to various scenarios, including changes in the number of antennas and angles of signal arrival. These findings suggest that the integration of artificial intelligence techniques into smart antenna systems holds great promise for addressing the challenges of today's dynamic and complex wireless communication environments. In conclusion, this research underscores the importance of continued innovation in smart antenna technology, with a particular focus on leveraging machine learning and deep learning to enhance DOA estimation and adaptive beamforming. As wireless communication continues to

evolve, these advancements will play a pivotal role in ensuring seamless connectivity and improved user experiences.

CONFLICT OF INTEREST STATEMENT

Authors declare that there is no conflict of interest for this work.

REFERENCES

1. Salhane, M. Rifi, H. Terchoune, S. Elmorabeti. Research, Design and optimization of smart beamforming Multiple patch antenna for microwave power transfer (MPT) for IoT applications. *2022 Int. Conf. Microelectron. ICM 2022* **2022**, 201–204.
2. R. Ullah, S. Ullah, R. Ullah, et al. Wideband and High Gain Array Antenna for 5G Smart Phone Applications Using Frequency Selective Surface. *IEEE Access* **2022**, 10, 86117–86126.
3. X.L. Chang, P.S. Chee, E.H. Lim, N.T. Nguyen. Frequency Reconfigurable Smart Antenna with Integrated Electroactive Polymer for Far-Field Communication. *IEEE Trans. Antennas Propag.* **2022**, 70 (2), 856–867.
4. V.P. Kodgirwar, S.B. Deosarkar, K.R. Joshi. Design of adaptive array with E-shape slot radiator for smart antenna system. *Prog. Electromagn. Res. M* **2020**, 90, 137–146.
5. R. Ullah, S. Ullah. 9-elements MIMO antenna system for 5G smartphone applications. *Wirel. Networks* **2021**, 2, 218477–218488.
6. N. Shoaib, S. Shoaib, R.Y. Khattak, et al. MIMO antennas for smart 5g devices. *IEEE Access* **2018**, 6, 77014–77021.
7. S.H. Kiani, A. Iqbal, S.W. Wong, et al. Multiple Elements MIMO Antenna System With Broadband Operation for 5th Generation Smart Phones. *IEEE Access* **2022**, 10, 38446–38457.
8. Y.Y. Wang, Y.L. Ban, Z. Nie, C.Y.D. Sim. Dual-loop antenna for 4G LTE MIMO smart glasses applications. *IEEE Antennas Wirel. Propag. Lett.* **2019**, 18 (9), 1818–1822.
9. L. Sun, Y. Li, Z. Zhang, Z. Feng. Wideband 5G MIMO Antenna with Integrated Orthogonal-Mode Dual-Antenna Pairs for Metal-Rimmed Smartphones. *IEEE Trans. Antennas Propag.* **2020**, 68 (4), 2494–2503.
10. M. Usman, E. Kobal, J. Nasir, et al. Compact SIW Fed Dual-Port Single Element Annular Slot MIMO Antenna for 5G mmWave Applications. *IEEE Access* **2021**, 9, 91995–92002.
11. P.K. Mohapatra, S.K. Rout, R.N. Panda, N.S. Gupta, N.K. Swain. Performance Analysis of Smart Antenna in Wireless Communication System. *Commun. Comput. Inf. Sci.* **2023**, 1861 CCIS, 256–265.
12. J. Romeu, S. Blanch, L. Pradell, et al. Lens-Based Switched-Beam Antenna for a 5G Smart Repeater. *IEEE Antennas Wirel. Propag. Lett.* **2023**, 22 (10), 2482–2486.
13. M. Wei, H. Zhao, V. Galdi, L. Li, T.J. Cui. Metasurface-enabled smart wireless attacks at the physical layer. *Nat. Electron.* **2023**, 6 (8), 610–618.
14. T.R. Dinesh Kumar, A. Karthikeyan. Proactive flow control using adaptive beam forming for smart intra-layer data communication in wireless network on chip. *Automatika* **2023**, 64 (4), 689–702.
15. R. Yadav, B.R. Dutta, S.K. Mishra, A.K. Johar, A. Tripathi. 3D MIMO beam forming using machine learning SVM algorithm for 5G wireless communication network. *AIP Conf. Proc.* **2023**, 2782 (1), 20018.
16. B. Biswas, D. Roy, M. Biswas. Designing a Broadband Antenna for Wireless Communication; Lecture Notes in Networks and Systems; Springer, Singapore, **2023**; Vol. 645 LNNS.
17. S. Komeylian, C. Paolini. Performance Evaluation of Implementing LCVM Beamformer for Cylindrical Antenna Array in Smart Array Antenna Applications. In *17th European Conference on Antennas and Propagation, EuCAP 2023*; Florence, Italy, **2023**; pp 1–5,.
18. P.P. Shome, T. Khan, A.A. Kishk, Y.M.M. Antar. Quad-Element MIMO Antenna System Using Half-Cut Miniaturized UWB Antenna for IoT-Based Smart Home Digital Entertainment Network. *IEEE Internet Things J.* **2023**, 10 (20), 17964–17976.
19. S. Bandewar, V.S. Chaudhary. Design and Analysis of Smart Antenna for Mobile Application. *SAMRIDDHI A J. Phys. Sci. Eng. Technol.* **2023**, 15 (01), 139–147.
20. M. Aboualalaa, I. Mansour, R.K. Pokharel. Energy Harvesting Rectenna Using High-Gain Triple-Band Antenna for Powering Internet-of-Things (IoT) Devices in a Smart Office. *IEEE Trans. Instrum. Meas.* **2023**, 72, 1–12.
21. A. Jabbar, Q.H. Abbasi, N. Anjum, et al. Millimeter-Wave Smart Antenna Solutions for URLLC in Industry 4.0 and Beyond. *Sensors* **2022**, 22 (7), 2688.